

Linewidth and DC properties of the flux-flow oscillator with mixed inline-overlap bias

A S Sobolev¹, J Mygind², V P Koshelets¹

¹ Institute of Radio Engineering and Electronics (IREE), Moscow, Russia

² Department of Physics, Technical University of Denmark, Kgs. Lyngby, Denmark

Corresponding author: Alexander Sobolev, e-mail: sobolev@hitech.cplire.ru

Abstract. A Flux-Flow Oscillator (FFO) is a long Josephson junction in which a unidirectional flow of magnetic flux quanta is maintained by an applied DC magnetic field and a bias current. In the overlap geometry the FFO voltage and thus its oscillation frequency is controlled independently by the (overlap) bias current and the so-called “control line” (inline) current, which creates the magnetic field at the ends of the FFO. We have studied both DC properties and the linewidth of the emitted radiation for an FFO, which can be biased in different ways; as a four current terminal object. The bias current of the mixed inline-overlap type is applied through the terminals commonly used for the “control line” current. In this configuration the bias current also contributes to the magnetic field at one of the two FFO ends. This changes the steepness of the junction’s I-V characteristics and therefore the bias current dynamic resistance. The experimental FFO linewidth was found to be independent of the bias configuration and determined by the dynamic resistance of the junction with pure overlap bias current. A new method has been developed to evaluate the difference in the DC magnetic field at the ends of the junction. It may be attributed to control line redistribution caused by the impedance matching RF circuit connected to the FFO at the end where the fluxon chain annihilates and radiation is emitted. We found that the opposite end, where the fluxons enter the junction, appears to be about three times more sensitive to variations of the magnetic field than the radiating end.

1. Introduction.

A flux-flow oscillator (FFO) is a long Josephson junction in which a viscous flow of magnetic flux quanta generates high frequency radiation emission. For more than a decade it has been considered to be the most best local oscillator for implementation in superconducting integrated receivers (SIRs) [1]. SIRs have been chosen for use in a collaborative European project on environmental monitoring. The SIR, which is being developed for the Terahertz Limb Sounder (TELIS) mission comprises on a single chip; the FFO as a local oscillator, a receiving antenna, an SIS-mixer and an SIS harmonic mixer as a part of the FFO phase locking loop (PLL). The SIR technology makes the device suitable for airborne missions, where compactness and low power consumption are vitally important. The autonomous linewidth of the FFO is one of the main characteristics, which along with noise temperature of the receiver defines its overall performance. An autonomous linewidth below 7 MHz is required to enable the FFO phase-locking by contemporary PLL systems with the spectral ratio between the phase-locked and the total FFO power better than 50% [2]. The FFO voltage is independently controlled by the two DC currents; one is referred to as “the control line” current, I_{CL} , which creates the magnetic field at the

two ends of the junction, while the bias current, I_B , applied through the tunneling barrier accelerates the Josephson vortices and moves them to the radiating end of the FFO. As indicated in Figure 1 there are one and three current terminals on the top and on the base FFO electrodes, correspondingly. Both terminals for I_{CL} are located on the same (base) electrode.

Previous studies [3] of the overlap type FFOs revealed that the linewidth Δf is given by Eq. (1), which along with the differential resistance Rd on the bias current I_B also contains the differential resistance Rd_{CL} the control line current I_{CL} :

$$\Delta f = 2\pi e \left(\frac{1}{\Phi_0} \right)^2 (Rd + K \cdot Rd_{CL})^2 \cdot \left[I_{QP} \coth \frac{eV}{2k_B T} + 2I_S \coth \frac{eV}{k_B T} \right] \quad (1)$$

This formula includes a nonlinear superposition of thermal and shot noise down-converted to low frequencies by the Josephson junction. I_{QP} and I_S are the quasi-particle and superconducting pair components of I_B , respectively. K - is a fitting parameter, depending mainly on the critical current density of the FFO and the geometry of its electrodes.

In this work we report on the experimental study of the Nb/AlOx/Nb junction with pure overlap geometry at various bias configurations using all three current terminals of the base electrode to apply the bias current. At certain bias configurations I_B also contributes to the magnetic field when injected into one of the FFO ends, in this case the Rd - value drastically changes together with the bias current distribution.

2. Experimental idea

A general 3D layout of the FFO being studied with the four current terminals is shown in Figure 1. Normally, terminals #1 and #2 on the base electrode are used for the control line current, while #3 and #4 provide the overlap bias configuration. The arrows on the sketch show the correct polarity for the currents I_B and I_{CL} when the magnetic vortices are moving towards the left FFO end to emit RF power into the transmission line, which starts from the impedance transformer, as shown in Figure 1.

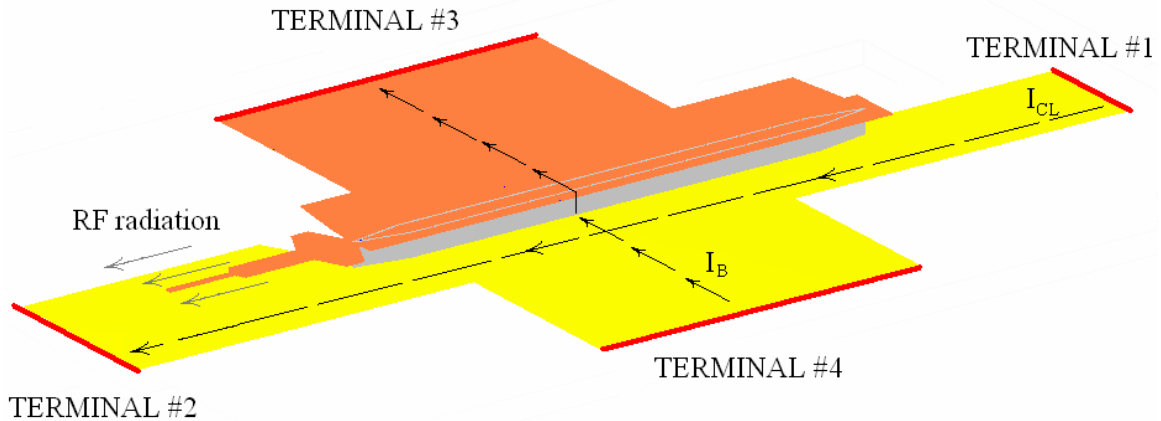


Figure 1. A simplified 3D layout of the FFO with the four current terminals.

Table 1 gives a description of how the FFO, as an object with four ports, can be connected to the two bias current sources. Connection #1 (pure overlap case) corresponds to the conventional bias, #2 and #3 provide the situation, where the magnetic field is created only at the end, where the flux quanta enter the FFO. With connection #2 the fluxons move in the direction of the terminal T2 towards the transmission line, but for #3 this motion is opposite. I_B makes a positive contribution to the magnetic field Γ_1 at the penetrating end for connection #4, while #5 corresponds to a negative contribution to the magnetic field Γ_2 at the radiating end. These two bias connections transform the junction into a mixed

overlap-inline type. The corresponding expressions for the magnetic fields Γ_1 and Γ_2 are contained in Table 1.

Table 1. Description of the bias connections and the corresponding expressions for the values of the magnetic field at the FFO ends.

Bias number	Terminal number for corresponding current connection				Magnetic field Γ_1 at the penetrating end	Magnetic field Γ_2 at the radiating end
	$+I_B$	$-I_B$	$+I_{CL}$	$-I_{CL}$		
#1	T4	T3	T1	T2	$\beta_1 I_{CL}$	$\beta_2 I_{CL}$
#2	T4	T3	T1	T4	$\beta_1 I_{CL}$	0
#3	T3	T4	T4	T2	0	$-\beta_2 I_{CL}$
#4	T2	T3	T1	T2	$\beta_1 (I_{CL} + I_B)$	$\beta_2 I_{CL}$
#5	T1	T3	T1	T2	$\beta_1 I_{CL}$	$\beta_2 (I_{CL} - I_B)$

Let's consider connection #5 as an example. Since both I_B and I_{CL} flow in the same path along the base electrode towards the terminal T2 the magnetic field at the FFO ends is defined by $\Gamma_1|_{\#5} = \beta_1 I_{CL}$; $\Gamma_2|_{\#5} = \beta_2 (I_{CL} - I_B)$.

Here β_1 and β_2 are proportionality coefficients between the field and the current running in the base electrode along the FFO. The negative field contribution reduces Rd , as compared to the conventional connection, while the positive contribution increases it.

3. Experimental results

The control line current running between the terminals T1 and T2 creates different magnetic field values Γ_1 and Γ_2 at the entrance end and at the radiating end. For our experiments we used Nb/AlOx/Nb junctions with $RnS = 37 \Omega \cdot \mu m^2$ (product of the normal state resistance and the junction area).

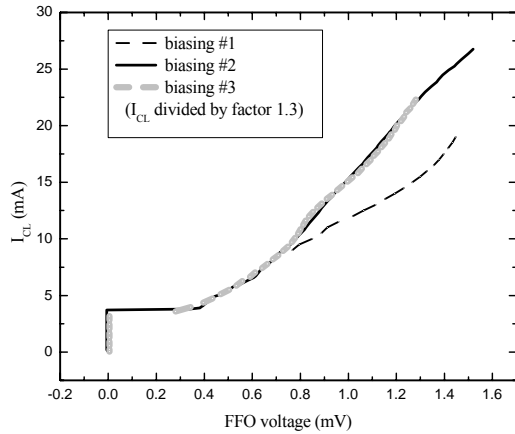


Figure 2. The dependence of I_{CL} on the FFO voltage for #1 (bars), #2 (black solid line), #3 (grey dashed line) divided by factor 1.3 for normalizing to #2

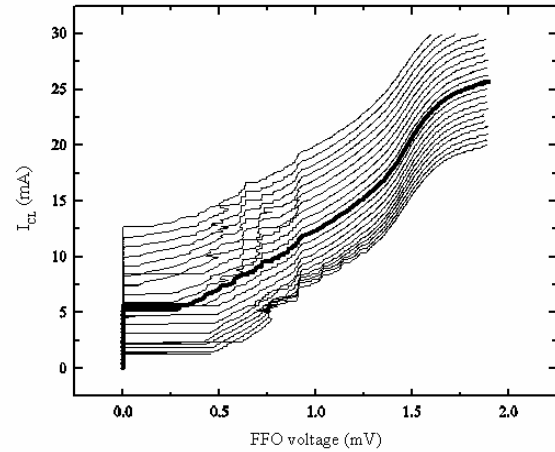


Figure 3. A family of voltage – control line current characteristics, measured at $I_B = 5$ mA for different I_{CL2} values in the range from -10 mA (top curve) to +10 mA (bottom curve) with 1 mA step. The thick line corresponds to $I_{CL2} = 0$.

Fig.2 shows the dependence of the I_{CL} on the FFO voltage V at constant $I_B = 6$ mA for connections #1 (black bars), #2 (black solid line) and #3 (dash-dot grey line). The third curve was scaled to the second one by normalizing I_{CL} by factor 1.3. This factor is a ratio between Γ_1 and Γ_2 for any I_{CL} , thus

we have $\beta_2/\beta_1 = 1.3$. Black bars correspond to the conventional bias, where the magnetic field is applied to the both FFO ends; with this connection the FFO voltage is larger for the same value of I_{CL} , as compared to connections #2 and #3 where the magnetic field is applied at one end only.

As a result of a mixed-type bias we have to deal with the situation when the total inline current, running in the bottom electrode is different for the two FFO ends. Therefore it is necessary to relate the conventional Rd_{CL} to the differential resistance Rd_{CLi} , when the control line I_{CLi} increments only at one FFO end:

$$Rd_{CLi} = \partial V / \partial I_{CLi} = \beta_i \partial V / \partial I_i \quad (2)$$

The subscript i can be equal to 1 or 2 for the penetrating or the radiating FFO ends, correspondingly. Assuming the ratio between Rd_{CL} and Rd_{CLi} to be linear:

$$Rd_{CLi} = A_i * Rd_{CL} \quad (3)$$

one can find the parameter A_i from DC tests. An additional current source was used to apply the second independent control line current ΔI_{CL} to one of the two junction's ends. It was used together with the main control line source whereas I_B sources where #1 connected.

In Figure 3 we give the family of the FFO IV-curves $V(I_{CL})$ measured at constant $I_B = 5\text{mA}$ for different values of ΔI_{CL} in the range $-10\dots+10\text{mA}$ with 1mA increment. The current ΔI_{CL} was applied between the terminals T1 and T4. The thick line corresponds to $\Delta I_{CL} = 0$. The curves below are measured with positive ΔI_{CL} , when the additional magnetic field at the penetrating end is unidirectional with the background field, created by I_{CL} . Negative values of ΔI_{CL} reduce both the magnetic field at the penetrating end and the DC FFO voltage, which shifts the IV-curve's family to the left from the thick curve. From these data Rd_{CL} , Rd_{CL1} and therefore the A_1 -coefficient at the corresponding fixed I_B can be found. The two curves in Figure 3 corresponding to $\Delta I_{CL} = 0$ and $\Delta I_{CL} = 1\text{mA}$ give the following $Rd_{CL}(V)$ and $Rd_{CL1}(V)$ dependence shown in Figure 4. Here $Rd_{CL}(V)$ (light gray curve) is multiplied by a factor 0.76 for scaling it to $Rd_{CL1}(V)$ (black curve). This factor is the exact experimentally found value of the A_1 -coefficient in Eq. (3).

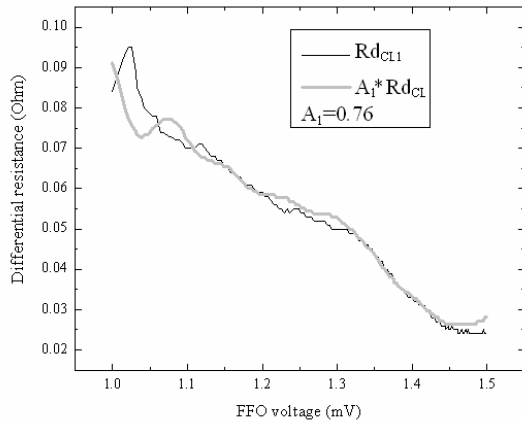


Figure 4. Rd_{CL} and Rd_{CL1} as function of the FFO voltage at constant $I_B = 5\text{mA}$. Rd_{CL} is multiplied by 0.76 to scale it to Rd_{CL1} . This means that the A_1 -parameter from Eq. (3) is equal to 0.76

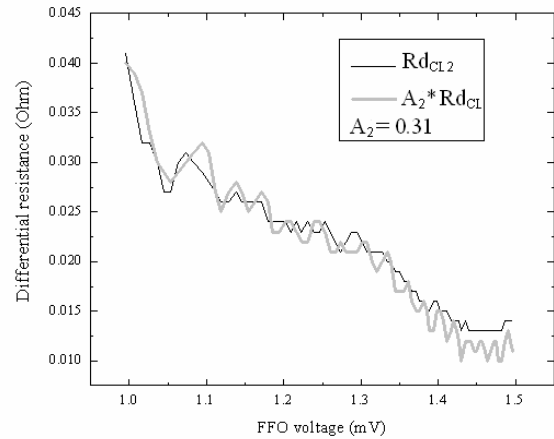


Figure 5. Rd_{CL} and Rd_{CL2} as functions of the FFO voltage at constant $I_B = 5\text{mA}$. Rd_{CL} is multiplied by 0.31 to scale it to Rd_{CL2} . This means that the A_2 -parameter from Eq. (3) is equal to 0.31

Figure 5 shows the similar data but obtained with ΔI_{CL} applied to the radiating end between the terminals T4 and T2, from which we find $A_2 = 0.31$. The sum $A_1 + A_2$ equals to 1.08 (very close to unity) and reflects the fact that $Rd_{CL} = Rd_{CL1} + Rd_{CL2}$

Now from Eq. (2) and the fact that $Rd_{CL} = Rd_{CL1}A_1^{-1} = Rd_{CL2}A_2^{-1}$ one find the ratio

$$\frac{\partial V}{\partial \Gamma_1} \left(\frac{\partial V}{\partial \Gamma_2} \right)^{-1} = \beta_2 A_1 (\beta_1 A_2)^{-1} = 3.18 \quad (4)$$

meaning that the FFO voltage is three times more sensitive to the magnetic field at the entrance end as compared to the radiating end.

4. FFO linewidth measurements

The FFO linewidth measurements were made in the frequency range 500 – 750GHz at the current $I_B=7$ mA. The data were fitted by the Eq. (1) with the K-factor as fitting parameter. For connections #4 and #5 the bias current I_B also contributes to the magnetic field and the differential resistance Rd was significantly changed compared to the conventional bias connection #1. As a result, the data points in Figure 6 corresponding to the different bias types are well separated. Curve A in Figure 6 fits the experimental data (bars) with $K \approx +0.1$ for connection #1. For curve B together with the experimental points (diamonds) corresponding to #5, the fitting gives $K \approx +0.25$. Curve C with the data points (stars) represents configuration #4, for which we obtain $K \approx -1.1$. A recent theory [4] in combination with the DC measurements described above can give very similar K-values. The theory is based on the assumption that the linewidth Δf of any Josephson oscillator, the voltage of which can be independently controlled by the both a bias current and a magnetic field, is determined only by internal bias current fluctuations. The differential resistance Rd' on the bias current is the only parameter converting current fluctuation with spectral density $S_I(\omega)$ into voltage fluctuations $S_V(\omega)$. This gives the well-known expression valid for the lumped Josephson element and wideband current fluctuations:

$$\Delta f = 2\pi e \left(\frac{1}{\Phi_0} \right)^2 (Rd')^2 \cdot \left[I_{QF} \coth \frac{eV}{2k_B T} + 2I_S \coth \frac{eV}{k_B T} \right] \quad (5)$$

When the bias current somehow contributes to the magnetic field and modifies the differential resistance the internal bias current fluctuations do not induce fluctuations in the magnetic field and thus the linewidth Δf does not change it's value. Nevertheless, in order to find Δf one should know $S_I(\omega)$ as in Eq. (1) and the Rd' -value of the “bare” junction i.e. a fictitious junction in which the magnetic field has no contribution from the bias current.

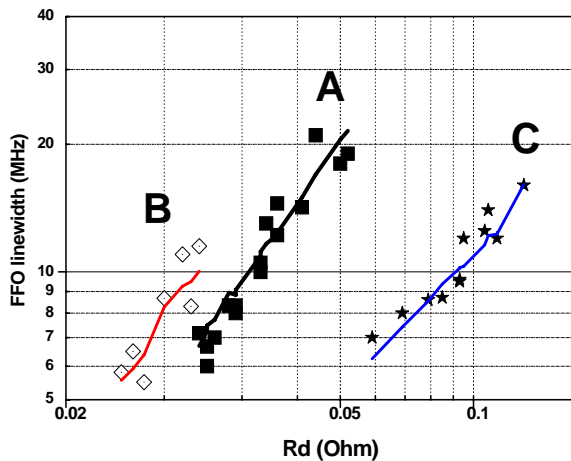


Figure 6. FFO linewidth represented as a function of the measured differential resistance on the bias current for pure overlap connection #1 (solid bars), overlap-inline connection with a negative contribution into the magnetic field #5 (diamonds), overlap-inline connection with a positive contribution #4 (stars).

In our experiments the FFO voltage is a function of I_B and the magnetic fields Γ_1 and Γ_2 , and it is possible to recover the “bare” Rd' from the differential resistance Rd measured for connections #4 and #5. For #1 the K-factor is close to zero, Eq. (1) transforms into Eq. (5) and the measured Rd -value is the “bare” differential resistance Rd' . The voltage of the “bare” FFO with the pure overlap bias is a

function $V = V(I_B, \Gamma_1, \Gamma_2)$, while, for example, for the bias #4 it takes the form $V_{\#4} = V_{\#4}(I_B, \beta_1(I_{CL} + I_B), \Gamma_2)$. In this case the measured dynamic resistance

$$Rd|_{\#4} = \frac{\partial V}{\partial I_B} + \beta_1 \frac{\partial V}{\partial \Gamma_1} = Rd' + Rd_{cl1} \quad (6)$$

Taking into account Eq. (2) and Eq. (3) we express Rd'

$$Rd' = Rd|_{\#4} - A_1 * Rd_{cl} \quad (7)$$

to be substituted into Eq. (5) for the linewidth of the lumped junction, which takes the form (1) with $K = -A_1 = -0.76$. In the same way we find

$$Rd' = Rd|_{\#5} + A_2 * Rd_{cl} \quad (8)$$

for the connection #5 with $K = A_2 = 0.31$. These theoretical estimations of the K -factor deviate from the experimental fitting (it gave the K -factor values equal to -1.1 and +0.25 for #4 and #5) by 30%, probably, due to the influence of the spatial redistribution of the bias current for different connection types and perhaps some noise conversion from the bias current into the magnetic field.

5. Conclusion

We have experimentally investigated the flux-flow oscillator biased in different configurations so that the bias current created an additional magnetic field at either the radiating or the penetrating end of the junction and therefore the differential resistance on this current was changed. Although the steepness of the FFO I-V curves was different for all the bias types it was found that the FFO linewidth did not drastically change compared to the case of the conventional pure overlap-type bias connection. The linewidth data for the mixed overlap-inline cases fit the equation previously used to describe the linewidth of the FFO biased as a purely overlap Josephson junction. Positive K -factor was obtained for the negative contribution to the magnetic field by the bias current, while a negative K -factor corresponded to a positive contribution. This result complies with a simple theory recently developed for the long Josephson junction.

6. Acknowledgements

The work was supported in parts by the RFBR projects 06-02-17206, the ISTC project # 3174, NATO SfP Grant 981415, the Grant for Leading Scientific School 7812.2006.2, and the Hartmann Foundation

References

- [1] P. Koshelets, S.V. Shitov, A.B. Ermakov, O.V. Koryukin, L.V. Filippenko, A. V. Khudchenko, M. Yu. Torgashin, P. Yagoubov, R. Hoogeveen, O.M. Pylypenko, *IEEE Trans. on Appl. Supercond.*, vol. **15**, pp. 960-963, 2005
- [2] V.P. Koshelets, A.B. Ermakov, L.V. Filippenko, A.V. Khudchenko, O.S. Kiselev, A.S. Sobolev, M.Yu. Torgashin, P.A. Yagoubov, R.W.M. Hoogeveen, and W. Wild, *IEEE Trans. on Appl. Supercond.*, vol. **17**, pp. 336-342, 2007
- [3] V. Koshelets, P. D. A. Ermakov, A. Sobolev, A. Baryshev, P. Wesselius, and J. Mygind, *Supercond.Sci. Tech.*, vol. **14**, pp. 1041–1045, 2001
- [4] J. Mygind, M. R. Samuelsen, V. P. Koshelets and A. S. Sobolev, *IEEE Trans. on Appl. Supercond.*, vol. **15**, pp. 968-971, 2005